



THE UNIVERSITY *of* EDINBURGH

Edinburgh Research Explorer

## Multihump thermo-reorientational solitary waves in nematic liquid crystals: Modulation theory solutions

**Citation for published version:**

Assanto, G, Khan, C & Smyth, NF 2021, 'Multihump thermo-reorientational solitary waves in nematic liquid crystals: Modulation theory solutions', *Physical Review A*, vol. 104, no. 1, 013526.  
<https://doi.org/10.1103/PhysRevA.104.013526>

**Digital Object Identifier (DOI):**

[10.1103/PhysRevA.104.013526](https://doi.org/10.1103/PhysRevA.104.013526)

**Link:**

[Link to publication record in Edinburgh Research Explorer](#)

**Document Version:**

Peer reviewed version

**Published In:**

Physical Review A

**General rights**

Copyright for the publications made accessible via the Edinburgh Research Explorer is retained by the author(s) and / or other copyright owners and it is a condition of accessing these publications that users recognise and abide by the legal requirements associated with these rights.

**Take down policy**

The University of Edinburgh has made every reasonable effort to ensure that Edinburgh Research Explorer content complies with UK legislation. If you believe that the public display of this file breaches copyright please contact [openaccess@ed.ac.uk](mailto:openaccess@ed.ac.uk) providing details, and we will remove access to the work immediately and investigate your claim.



# Multi-hump thermo-reorientational solitary waves in nematic liquid crystals: Modulation theory solutions

Gaetano Assanto,<sup>1</sup> Cassandra Khan,<sup>2</sup> and Noel F. Smyth<sup>3</sup>

<sup>1</sup>**NooEL**— *Nonlinear Optics and OptoElectronics Lab*  
*University of Rome “Roma Tre”, 00146 Rome, Italy*

<sup>2</sup>*School of Mathematics, University of Edinburgh, Edinburgh EH9 3FD, Scotland, U.K.*

<sup>3</sup>*School of Mathematics, University of Edinburgh, Edinburgh EH9 3FD, Scotland, U.K. and*  
*School of Mathematics and Applied Statistics, University of Wollongong,*  
*Wollongong, New South Wales, Australia, 2522.*

The propagation of light induced thermo-reorientational solitary waves in nematic liquid crystals is studied using numerical solutions of the full governing equations and variational approximations. These thermo-reorientational solitary waves form as the nonlocal refractive index response to extraordinarily polarized light beams is both self-focusing via the induced rotation of the constituent molecules and self-defocusing owing to the temperature increase through optical absorption. These competing nonlinearities can lead to the formation of one- and two-dimensional multi-humped solitary and ring-shaped waves at high enough optical powers, with a volcano profile in the plane transverse to propagation. The variational solutions for these self-localized structured beams are in remarkably good agreement with full numerical solutions of the governing equations.

PACS numbers: 42.65.Tg, 42.70.Df, 05.45.Yv

## I. INTRODUCTION

Nematic liquid crystals (NLC) have been considered an ideal platform for investigating the propagation of nonlinear bulk waves [1, 2] since the experimental demonstration of optical solitary waves or spatial solitons, termed nematicons, in such a medium [3]. Indeed, intense light beams in NLC display many of the classical properties of nonlinear dispersive waves and solitary wave bearing nonlinear dispersive wave equations, being modelled by a coupled system consisting of a nonlinear Schrödinger (NLS)-type equation for the propagating wavepacket and an elliptic equation for the medium response [1, 4, 5]. Moreover, NLC are a nonlocal optical medium, which means that its elastic response extends far beyond the transverse size of the optical forcing [1, 5, 6]. If sufficiently strong, the nonlocality can prevent the catastrophic collapse of  $(2 + 1)$  dimensional solitary waves governed by NLS-type equations above a power threshold [7, 8], including for nonlinear light beams in NLC [1, 5, 9]. At a mathematical level, the resulting stability derives from the elliptic character of the partial differential equation modelling the NLC response, so that its solution at any given location depends on the light field over the whole domain, rather than just at that point, as for a local medium [10].

The nonlinear reorientational response of NLC to extraordinarily polarized light beams stems from the electric field inducing dipoles in the constituent elongated molecules: their dipolar reaction causes them to rotate until the elastic forces balance the electromagnetic torque, thereby changing the refractive index of the corresponding eigenwaves [1–3]. If the refractive index increases, then the medium is self-focusing and can support bright solitary waves with an intensity rise above the background. If the index decreases, then

the medium is self-defocusing and dark solitary waves can form, which are dips in the intensity background [7]. When the dipoles are uniformly aligned in a plane transverse (orthogonal) to the beam wavevector, their nonlinear reorientation can cause polarization evolution of the incoming wavepacket and a resulting geometric phasefront [11], yielding “spin-optical” bright solitary waves [12–14].

Configurations for which the medium is subject to light-induced refractive index changes, in particular, raise the possibility that in the presence of competing optical nonlinearities with focusing and defocusing nonlocal responses, multi-peaked solitary waves can exist as defocusing pulls the beam away from the solitary wave axis, while focusing pulls it back in. An equilibrium between these components is expected to support multi-humped or “supermode” solitary waves [15–20].

The full  $(2 + 1)$  dimensional equations governing supermode solitary waves form a coupled system consisting of the optical equation, an NLS-type equation, and elliptic equations for the nematic and thermal responses [5]. As such, the determination of thermo-reorientational nematicon solutions of this coupled system is difficult, noting that even in the absence of thermal effects, there are no known general solutions of the nematic equations besides isolated solutions for fixed parameter values [10]. For this reason previous studies of thermo-reorientational nematicons have relied on simplified models of the full equations, often encompassing non-physical medium responses. The most popular of the latter for thermo-reorientational optical solitons in nonlocal, cubic media with competing nonlinearities is the general equation

$$i\frac{\partial u}{\partial z} + \frac{1}{2}\frac{\partial^2 u}{\partial x^2} + u \int_{-\infty}^{\infty} R(x-x')|u(x',z)|^2 dx' = 0, \quad (1)$$

where the kernel  $R$  encompasses the material nonlocality. If we set

$$R(x) = \chi_1 R_1(x) - \chi_2 R_2(x), \quad (2)$$

with  $\chi_1, \chi_2 \in \mathfrak{R}^+$ , then the model describes competing responses of opposite signs [16–18, 21]. The most often adopted kernel is the Gaussian  $R_i(x) = e^{-\beta_i x^2}$  in  $(1+1)$  dimensions, as it simplifies the calculations, particularly for variational approximations [15]. However, there is no known physical medium which possesses this Gaussian response. With these caveats, equation (1) with competing nonlinearities supports multi-humped solitary waves [16–18, 20], as their formal existence is not directly related to the specific response of a material system. Noteworthy, it was underlined that two-humped “supermode” solitary waves are fundamental solitary waves, inasmuch as their phase is constant across the whole transverse profile [19]. It was also predicted that, in the case of interacting bell-shaped solitary waves, either coherent or incoherent, competing nonlocal nonlinearities would result in attraction/repulsion with small/large separation between the beams, depending on the prevailing component in the nonlinear potential [15].

The general results for  $(1+1)$ D multi-humped solitary waves in media with competing nonlinearities have been specialized in several studies to the physics of NLC [19, 20], where the main contributions to changes in refractive index are the rotation of the molecular dipoles induced by the propagating light beam and the thermo-optic effect via weak linear (one photon) absorption [20, 22–24]. The latter dependence on temperature can be tailored by suitable dye-doping, allowing photon energy be absorbed from the beam and converted to heat [22, 25–28]. In these investigations of NLC, analytical studies were based on Gaussian approximations to the actual nematic reorientational and thermal responses [20], with numerical solutions required to determine supermode nematicons of the full system of equations [19]. However, the NLC reorientational response is of the form  $e^{-\beta|x|}$  in  $(1+1)$  dimensions and  $K_0(\beta r)$  in  $(2+1)$  dimensions, with  $K_0$  the modified Bessel function of the second kind of order 0, and the thermal response is of the forms  $(L - |x|)/\tau$  and  $\ln r/\tau$  in  $(1+1)$  and  $(2+1)$  dimensions, respectively. Hence, the (competing) reorientational and thermal responses of nematic liquid crystals are not of the same type, as commonly assumed when employing the model equation (1).

On a related topic, NLC have been shown to stabilize optical vortex propagation owing to either nonlinear reorientation or the thermo-optical effect [29, 30]. At variance with bell-shaped solitary waves, in fact, the stable propagation of optical vortices with a phase singularity and a dark core on-axis in nonlocal, nonlinear dielectrics is rather difficult to achieve [5].

In this Paper we investigate multi-humped  $(1+1)$ D as well as  $(2+1)$ D solitary waves in thermo-reorientational nematic liquid crystals, using a combination of numerical solutions of the full governing equations and modulation

theory [4, 31]. At variance with earlier analyses [19, 20, 25], we base our results on the full, physical nonlocal, nonlinear medium responses to optical forcing and temperature. In particular, the analytical thermo-reorientational nematicon solutions derived from modulation theory are found from the full equations, not the simplified models (1). Furthermore, by extending the analysis to two transverse dimensions, we reveal stable  $(2+1)$ D solitary wave solutions with a volcano shape, not addressed in previous work on such waves. As noted, even if thermal effects and nonlinear competition are neglected, the system governing light beams in NLC possesses no general solitary wave, or other solutions, except for specific fixed parameter values [10]. In such instances, variational and numerical solutions have been found to perfectly match with one another and provide excellent agreement with measurements if the trial functions on which variational methods are based are chosen suitably [5, 31–33]. Our previous work on the temperature control of nematicon trajectories, based on modulation theory, showed remarkable agreement [34] with the experimental results of [23, 24, 28], giving further verification of its applicability, with particular reference to the present work. Numerical thermo-reorientational nematicons are found using the imaginary time iteration method (ITEM) [35, 36]. This approach for solitary wave solutions of NLS-type equations only converges to linearly stable solutions, a great benefit unavailable from other methods, such as the Newton conjugate gradient method [37]. Therefore, both  $(1+1)$ D and  $(2+1)$ D thermo-reorientational nematicon solutions presented here are stable; the latter attribute enhances the expectation for their experimental demonstration.

## II. THERMO-REORIENTATIONAL EQUATIONS IN NLC

Let us consider the propagation of a coherent, linearly polarized light beam through a thick, transparent planar cell filled with liquid crystals in the nematic (fully oriented) metastate, with molecular director aligned to the down cell direction  $Z$  and the coordinates  $(X, Y)$  orthogonal to this. A beam of central wavenumber  $k_0$  is launched with wavevector  $\vec{k}_0$  in the  $Z$  direction, polarized so that its electric field  $E$  in air oscillates along  $Y$  and couples to extraordinary waves in the principal plane  $(Y, Z)$  of the uniaxial medium, with optic axis corresponding to the director [1, 3]. For mathematical convenience, we assume that a pre-tilting low frequency electric field  $E_{lf}$  is applied in the  $Y$  direction to preset the elongated molecules of the NLC at a finite angle  $\theta_0$  to  $Z$  and so overcome the Fréedericksz’ threshold [3, 38]. The NLC director is reoriented in the plane  $(Y, Z)$  by an addition angle  $\theta$  in the presence of intense light, so that its total angle becomes  $\psi = \theta_0 + \theta$  with respect to  $Z$ . The refractive index eigenvalues for electric fields  $E$

parallel and perpendicular to the optic axis are  $n_{\parallel}$  and  $n_{\perp}$ , respectively, so that the dielectric anisotropy is  $\epsilon_a = n_{\parallel}^2 - n_{\perp}^2 > 0$ . These refractive indices are taken to depend on the temperature  $T$ , see [23, 24, 28] for these measured dependencies for the common NLC mixture E7. In the paraxial, slowly varying envelope approximation the dimensional equations governing beam propagation in such an NLC sample are then [1, 17, 19, 20, 25, 27, 34]

$$2ik_0 n_e \frac{\partial E}{\partial Z} + \nabla^2 E + k_0^2 \left[ n_{\perp}^2 \cos^2 \psi + n_{\parallel}^2 \sin^2 \psi - n_{\perp}^2 \cos^2 \theta_0 - n_{\parallel}^2 \sin^2 \theta_0 \right] E = 0 \quad (3)$$

for the electric field  $E$  of the beam,

$$K \nabla^2 \psi + \frac{1}{2} \Delta \epsilon_{RF} E_{if}^2 \sin 2\psi + \frac{1}{4} \epsilon_0 \epsilon_a |E|^2 \sin 2\psi = 0 \quad (4)$$

for the reorientational response and

$$S \nabla^2 \tau = -\alpha \Gamma |E|^2, \quad \Gamma = \frac{1}{2} \epsilon_0 c n_e. \quad (5)$$

for the thermal response. The Laplacian  $\nabla^2$  is in the transverse variables  $(X, Y)$ . The parameter  $\Delta \epsilon_{RF}$  is the low frequency anisotropy of the medium. The temperature equation (5) does not depend on the longitudinal coordinate  $Z$  due to the large contrast between the longitudinal and transverse dimensions of typical cells [1], so that the heat flow is predominantly in the transverse plane. In Eq. (5)  $S$  is the thermal conductivity and  $\alpha$  the thermal absorption coefficient of the NLC, weakly doped so that Eq. (3) can be cast in a non-dissipative fashion. Finally, the refractive index  $n_e$  for extraordinarily polarized waves is given by

$$n_e^2 = \frac{n_{\perp}^2 n_{\parallel}^2}{n_{\parallel}^2 \cos^2 \psi + n_{\perp}^2 \sin^2 \psi}. \quad (6)$$

Note that a term  $i \Delta E_y$  describing the Poynting vector walk-off has not been included in the electric field equation (3). When the walk-off  $\Delta$  is a constant or has a negligible dependency on  $E$  and/or  $T$ , this term can be eliminated by a phase transformation of the electric field [39]. In addition, and more importantly for the present work, the solitary wave (nematicon) profile in NLC does not depend on the walk-off.

To simplify the subsequent analysis, the governing equations (3)–(5) will be set in non-dimensional coordinates  $(x, y, z)$  and non-dimensional electric  $u$  and temperature  $\tau$  fields using the transformations

$$\begin{aligned} Z &= L_z z, & X &= W x, & Y &= W y, & E &= A_b u, \\ T &= T_0 + A_T \tau. \end{aligned} \quad (7)$$

If we assume that the input beam is Gaussian, with power  $P_b$ , width  $W_b$  and amplitude  $A_b$ , then we have that [34]

$$A_b^2 = \frac{2P_b}{\pi \Gamma W_b^2}. \quad (8)$$

We set  $T_0$  to be the NLC temperature in the absence of the beam and a typical temperature rise to be  $A_T$  due to light. The subscripts  $t$  will refer to the quantities evaluated at the initial temperature  $T_0$ . Suitable length scales are therefore [34]

$$L_z = \frac{4n_e}{(\epsilon_a)_t k_0 \sin 2\theta_0}, \quad W = \frac{2}{k_0 \sqrt{(\epsilon_a)_t \sin 2\theta_0}}. \quad (9)$$

The non-dimensional equations governing the propagation of the optical wavepacket through the NLC become [1, 5, 6, 34]

$$i \frac{\partial u}{\partial z} + \frac{1}{2} \nabla^2 u + 2f(\tau)\theta u = 0, \quad (10)$$

$$\nu \nabla^2 \theta - 2q\theta = -2f(\tau)|u|^2, \quad (11)$$

$$\mu \nabla^2 \tau = -|u|^2. \quad (12)$$

The medium non-dimensional elasticity is

$$\nu = \frac{8K}{\epsilon_0 (\epsilon_a)_t A_b^2 W^2 \sin 2\theta_0}, \quad (13)$$

its non-dimensional thermal diffusivity is

$$\mu = \frac{S A_T}{\alpha \Gamma W^2 A_b^2} \quad (14)$$

and the non-dimensional (externally applied) pre-tilting electric field is

$$q = \frac{2\Delta \epsilon_{RF} E_{if}^2 \sin 2\theta_0}{\epsilon_0 \epsilon_a A_b^2 \theta_0}. \quad (15)$$

The function  $f(\tau)$  in Eqs. (10)–(11) encompasses their coefficient variations due to the temperature dependencies of  $n_{\parallel}$  and  $n_{\perp}$ , as in previous work [19, 20, 25].

The full system of thermo-optic nematic equations (10)–(12) does not possess a Lagrangian formulation for arbitrary  $f(\tau)$ . However, if the temperature  $\tau$  is a known function of  $(x, y, z)$ , then these equations have the Lagrangian formulation [34]

$$\begin{aligned} L &= i(u^* u_z - u u_z^*) - |\nabla u|^2 + 4f(\tau)\theta |u|^2 \\ &\quad - \nu |\nabla \theta|^2 - 2q\theta^2. \end{aligned} \quad (16)$$

The dependence of the NLC refractive indices on temperature is an order of magnitude less than on the director orientation [20, 22, 23, 38]. Experimental measurements indicate that, for the standard NLC mixture E7, the refractive index eigenvalues  $n_{\parallel}$  and  $n_{\perp}$  have a nearly linear variation with temperature up to around  $40^\circ\text{C}$ , after which the variation picks up additional quadratic and cubic temperature dependence up to  $55^\circ\text{C}$  [23, 34]. Between  $20^\circ\text{C}$  and  $40^\circ\text{C}$ ,  $n_{\parallel}$  decreases by around 0.6% and  $n_{\perp}$  increases by about 1.3%, so the temperature dependence is weak, as stated. It is assumed hereby that the refractive indices vary linearly with temperature from the background value  $T_0$

and that  $f(\tau)$  can be expanded in a Taylor series to second order as  $f(\tau) = 1 - \gamma\tau$ , where  $\gamma$  is related to  $f'(0)$  as  $T = T_0$  gives  $\tau = 0$ . The minus sign is due to the defocusing opto-thermal response [19, 20, 23, 25, 34], with the thermo-optic and reorientational optical nonlinearities in competition.

Next, the existence of two humped thermo-reorientational nematicons governed by the system (10)–(12) will be studied with the aid of numerical solutions and modulation theory [4, 5]. This analysis will be performed for solitary waves which are either one or two dimensional in the transverse plane, that is, (1 + 1)D and (2 + 1)D thermo-reorientational nematicons. These structured nematicons derived from modulation theory will be compared with steady solutions of the full NLC equations (10)–(12) obtained from the accelerated imaginary time evolution method (ITEM) [35, 36]. As stated above, the latter only converges to (linearly) stable solitary wave solutions of NLS-type equations. Hence, the presented numerical thermo-reorientational nematicons are guaranteed to be stable, which gives confidence for their forthcoming experimental observation.

### III. (1 + 1) DIMENSIONAL SOLUTIONS

Let us first consider the case of (1 + 1) dimensional thermo-reorientational nematicons, so that the beam is a function of  $(y, z)$ . As noted above, the NLC equations (10) and (11) in the case of temperature independent parameters have no known general exact solitary wave solutions, let alone more involved travelling wave solutions, except isolated cases for fixed parameter values [10]. As a consequence, variational methods are useful if the trial functions used are chosen appropriately to give good approximations to the actual solution, as they then provide outcomes in excellent agreement with full numerical solutions and experimental results [5, 31, 32]. These approaches are an extension of solitary wave perturbation theory [40] to include approximations to unknown solitary wave solutions. Gaussian trial functions have been found appropriate for studying nematicons [5], particularly as the coherent light beams used in most experiments have a Gaussian intensity profile. Here, we shall use Gaussian profiles for the beam electric field and the resulting director distribution

$$u = a \left[ e^{-(y-\xi)^2/w^2} + e^{-(y+\xi)^2/w^2} \right] e^{i\sigma}, \quad (17)$$

$$\theta = \alpha \left[ e^{-(y-\xi)^2/\beta^2} + e^{-(y+\xi)^2/\beta^2} \right]. \quad (18)$$

In the present work we are interested in steady state nematicons, so that the electric field amplitude  $a$  and width  $w$  and the director amplitude  $\alpha$  and width  $\beta$  are assumed constant. The electric field phase  $\sigma$  is a function of  $z$ , which will be found to be linear, as for the NLS equation solitons [4].

As stated above, the Lagrangian (16) is only valid for the temperature dependent NLC system if the temperature dependence  $\tau$  is a known function of  $(y, z)$ . The trial function (17) for the electric field can be used to solve the temperature equation (12), which is

$$\mu \frac{\partial^2 \tau}{\partial y^2} = -|u|^2 = -a^2 \left[ e^{-(y-\xi)^2/w^2} + e^{-(y+\xi)^2/w^2} \right]^2 \quad (19)$$

in (1 + 1) dimensions. While this equation can be solved in terms of integrals of error functions, this solution is of little use in averaging the Lagrangian (16), which is the basis of modulation theory [4], as the latter needs to be integrated in  $y$  from  $-\infty$  to  $\infty$  [4]. Since our aim is to find multi-hump thermo-reorientational nematicons, the humps can be assumed well separated with  $\xi$  relatively large,  $\xi > w$ . This assumption will be verified from numerical and variational solutions. We take the NLC sample to have a non-dimensional width  $2L$  and a temperature fixed at the background value at the cell boundaries, i.e.,  $\tau = 0$  at  $x = \pm L$ . The thermal diffusivity  $\mu$  given by (14) is  $O(100)$  for typical experimental parameters [34]; therefore, the temperature is expected to be nearly the constant  $\tau_0$  between the nematicon peaks due to the enhanced heat flow. Away from the exponentially decaying beam profile, the temperature is a solution of the homogeneous form of (26), so that the temperature is linear. On satisfying the boundary condition, we then approximate the temperature by

$$\tau = \begin{cases} \frac{\tau_0(L-|y|)}{L-\xi}, & \xi < |y| \leq L, \\ \tau_0, & 0 \leq |y| \leq \xi. \end{cases} \quad (20)$$

This approximation will be checked by comparisons with numerical solutions.

To determine  $\tau_0$ , let us integrate the temperature equation (19) from  $y = 0$  to  $y = L$ , yielding

$$\mu \frac{\partial \tau}{\partial y} \Big|_{y=L} = -\frac{\sqrt{\pi}}{\sqrt{2}} a^2 w \left[ 1 + e^{-2\xi^2/w^2} \right] \quad (21)$$

on using the symmetry of the temperature profile about  $y = 0$ . This gives the slope of the temperature solution away from the beam, so that

$$\tau_0 = \frac{\sqrt{\pi}}{\sqrt{2}\mu} a^2 w (L - \xi) \left[ 1 + e^{-2\xi^2/w^2} \right] \quad (22)$$

on applying the boundary condition at  $y = L$  and the continuity of the temperature (20) at  $y = \pm \xi$ .

Having derived the temperature in terms of the power  $a^2 w$  of the light beam, the trial functions (17) and (18) can be used to calculate the averaged Lagrangian from which the variational approximation to the thermo-reorientational solitary wave can be determined. These trial functions are substituted into the Lagrangian (16), which is then averaged by integrating in  $y$  over the cell [4]. As  $L \gg \xi$ , as discussed above, the averaging

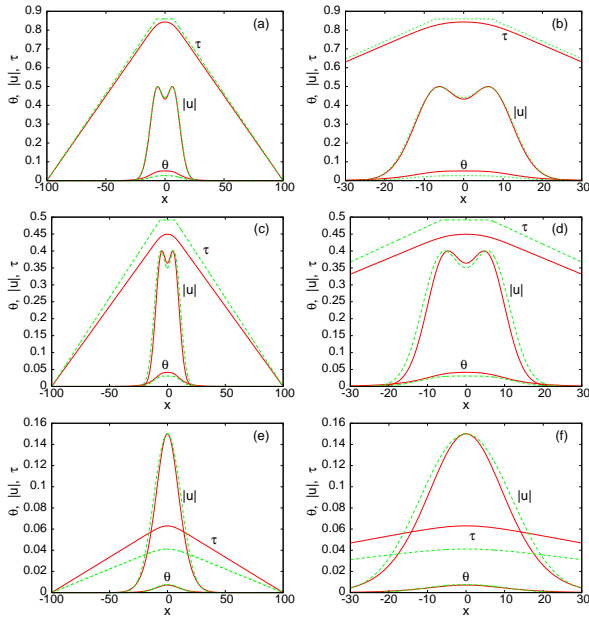


FIG. 1: Comparison between the  $(1 + 1)$ D thermo-reorientational solitary wave given by solutions of the nematic equations (10)–(12) and solutions of the  $(1 + 1)$ D modulation equations (A1)–(A5). Solution of nematic equations: red (full) line; modulation solution: green (dashed) line. (a) Amplitude  $a = 0.5$ , with detailed view in (b), (c) amplitude  $a = 0.4$ , with detailed view in (d), (e)  $a = 0.15$ , with detailed view in (f). Here,  $\nu = 200$ ,  $\mu = 300$ ,  $q = 2$  and  $\gamma = 0.5$ .

is performed from  $-\infty$  to  $\infty$  to easily compute the integrals. The calculation of this averaged Lagrangian is straightforward, although tedious, except for the average of  $f(\tau)\theta|u|^2$ , in particular that of  $\gamma\tau\theta|u|^2$ . Since the trial functions decay exponentially away from the symmetric peaks at  $y = \pm\xi$ , to average  $\tau\theta|u|^2$  we take  $\tau$  to be  $\tau_0$  over the beam, which is exact for  $|y| \leq \xi$ , but just an approximation for  $|y| > \xi$ . In this manner, the averaged Lagrangian can be determined as

$$\begin{aligned}
\frac{1}{\sqrt{\pi}}\mathcal{L} = & -2\sqrt{2}a^2w\sigma' \left[ 1 + e^{-2\xi^2/w^2} \right] \\
& -\sqrt{2}\frac{a^2}{w} \left[ 1 + \left( 1 - \frac{4\xi^2}{w^2} \right) e^{-2\xi^2/w^2} \right] \\
& -\sqrt{2}\nu\frac{\alpha^2}{\beta} \left[ 1 + \left( 1 - \frac{4\xi^2}{\beta^2} \right) e^{-2\xi^2/\beta^2} \right] \\
& -2\sqrt{2}q\alpha^2\beta \left[ 1 + e^{-2\xi^2/\beta^2} \right] \\
& + \frac{8\alpha a^2\beta w}{\sqrt{2\beta^2 + w^2}} \left[ 1 + e^{-\frac{8\xi^2}{2\beta^2 + w^2}} + 2e^{-\frac{4(\beta^2 + w^2)\xi^2}{w^2(2\beta^2 + w^2)}} \right] \\
& + \frac{8\gamma\tau_0\alpha a^2\beta w}{\sqrt{2\beta^2 + w^2}} \left[ 2 + e^{-\frac{4(\beta^2 + w^2)\xi^2}{w^2(2\beta^2 + w^2)}} \right]. \quad (23)
\end{aligned}$$

The modulation equations to obtain the variational approximation to the thermo-reorientational nematicon

solution are now found by taking variations of the averaged Lagrangian (23) with respect to the nematicon parameters  $a$ ,  $w$ ,  $\alpha$ ,  $\beta$ ,  $\sigma$  and  $\xi$ . These modulation equations, detailed in Appendix A, form a system of algebraic equations determining the parameters of the thermo-reorientational nematicon. These equations are based on the interaction of the two Gaussian beams in (17) and (18), so they are rather involved, as in previous work on interacting nematicons [39, 41, 42]. Nevertheless, as in these earlier studies, these variational solutions provide insight into the basic structure of the thermo-reorientational nematicons and the competition between the focusing reorientational and the defocusing thermal nonlinearities. Care needs to be adopted in solving the variational equations as there are multiple roots, most of which are non-physical or not relevant for the multi-humped solutions we seek. Examples of improper roots are solutions with negative amplitude and those with nematicon attached or too close to the cell edge, rather than centered at  $y = 0$ . The latter would be surface waves, are not of interest here, see [43, 44] for a discussion of surface thermo-optical solitary waves. For these reasons, Newton's method was not found suitable for solving the algebraic equations as did not allow enough control over the root to which it converged. An extension of Newton's method, the Broyden's method [45, 46], was found appropriate to obtain relevant roots of the modulation equations due to its flexibility. Even with the latter, however, the initial guess had to be close to the root for convergence to a valid solution. Such proper guesses were informed by the full numerical solution stemming from the imaginary time evolution method. Indeed, the ITEM method would also converge to the same non-physical solutions (surface waves etc) if the initial guess were not close enough to the required solution. In practice, to obtain good initial guesses for both Broyden's method and the ITEM, they had to be interplayed to provide good initial guesses for each method, that is both methods were needed to obtain the required thermo-reorientational nematicons. Broyden's method was also employed to solve the modulation equations for the  $(2 + 1)$ D thermo-reorientational nematicons dealt with in the next section, with the same caveats regarding appropriate choices for the initial guesses for it and the ITEM. The final point is that the amplitude of the thermo-reorientational solitary wave can be set to a given  $a^*$  with the imaginary time evolution method. To compare solutions of the modulation equations with these numerical ones, the amplitude  $a$  of the trial function (17) needs to be adjusted so that the total amplitude of  $|u|$  is  $a^*$ .

Figure 1 compares  $(1 + 1)$ D steady thermo-reorientational solitary wave solutions of the full NLC equations (10)–(12) and those of the modulation equations (A1)–(A5) derived from the  $(1 + 1)$ D averaged Lagrangian (23). Displayed are the electric field  $|u|$ , the director angle  $\theta$  and the temperature  $\tau$  for the

beam amplitudes  $a = 0.5, 0.4, 0.15$ , respectively. Overall there is excellent agreement between the numerical and modulation solutions, with a flat phase distribution confirming their solitary wave character. Figs. 1(a)–(d) show self-localized light beams with a “volcano,” multi-hump shape, while the director distribution has a single hump. This is due to the large nonlocality parameter  $\nu = 200$ , resulting in a highly nonlocal response which smooths out the two-humped material response. As the optical intensity reduces, the thermal response given by (12) also decreases, weakening the defocusing versus the focusing reorientation. As the amplitude reduces, the width and depth of the “volcano” in the thermo-reorientational beam decrease. At a critical amplitude, critical beam intensity, the beam becomes single humped due to the defocusing (thermal) response not being sufficiently strong. The numerical imaginary time evolution method yields the critical amplitude  $a = 0.21$  for the onset of a single humped beam, whereas modulation theory provides the critical amplitude  $a = 0.24$  for the parameters given in the caption of Fig. 1. Figures 1(a)–(d) present solutions above these critical values, while Figs. 1(e) and (f) show a solution below this critical intensity. It is also noted that the assumed temperature solution form (20) is in very good agreement with its numerical profile, which validates the approximations used to derive it.

It can be seen from Fig. 1 that, as the beam amplitude  $a$  and its intensity decrease, the agreement between numerical and modulation solutions for the temperature  $\tau$  deteriorates. This is because the approximate solution (20) given by Eq. (12) is based on a large separation between the beam maxima. However, this separation goes down with the optical intensity, invalidating this assumption. Given this, it is remarkable how accurate the modulation solution is for  $a = 0.15$  in Figs. 1(e) and (f). It should be noted that the modulation solution gives the separation  $\xi = 5.5$  and width  $w = 14$  in this case, so that the two beams of the trial functions (17) and (18) are not centred at the origin. The profile appears single peaked as the separation is significantly less than the width.

As stated above, the modulation equations of Appendix A are involved due to the trial functions relying on two interacting beams, but they can provide insight into the existence of multi-humped nematicons. The key equation in this regard is (A4), the variational equation due to variations  $\delta\xi$ , which arises for two interacting beams with non-zero separation  $\xi$ . The nematicon phase is  $\sigma' > 0$ . For this modulation equation to have a valid solution, the temperature effect  $\gamma\tau_0$  (due to the defocusing response) needs to overcome the other terms with the opposite sign. Moreover, the separation  $\xi$  needs to be large enough for the same reason. These observations and deductions give a basis for the detailed results visible in Fig. 1.

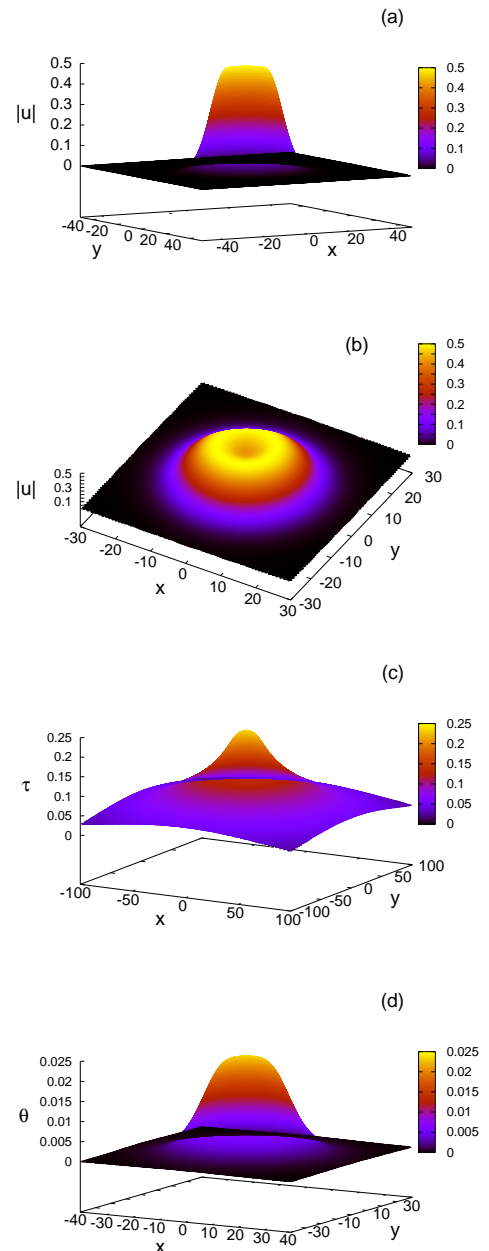


FIG. 2: Numerical solutions of the  $(2 + 1)$ D NLC equations (10)–(12) for an electric field amplitude  $a = 0.5$ . Three-dimensional rendering of (a-b) the electric field magnitude  $|u|$ , corresponding (c) temperature distribution  $\tau$  and (d) director angle distribution  $\theta$ . Here,  $\nu = 200$ ,  $\mu = 300$ ,  $q = 2$  and  $\gamma = 3.0$ .

#### IV. $(2 + 1)$ DIMENSIONAL SOLUTIONS

The investigation of  $(1 + 1)$ D multi-humped thermo-reorientational nematicons of Section III will now be extended to  $(2 + 1)$ D. These thermo-reorientational nematicons are radially symmetric, with a volcano shape due to the central dip. As for the  $(1 + 1)$ D case, the

modulation solutions will be found based on the actual reorientational and thermal responses of the NLC, not simplified and/or unphysical models. The numerical thermo-reorientational nematicons in (2 + 1)D will be determined using the ITEM in order to guarantee their linear stability.

As the calculation of the averaged Lagrangian in (2 + 1)D is similar to (1 + 1) dimensions, only an outline will be presented. The solitary wave beam is assumed radially symmetric, so the Gaussian trial functions for the electric field and director distribution are

$$u = a \left[ e^{-(r-\xi)^2/w^2} + e^{-(r+\xi)^2/w^2} \right] e^{i\sigma}, \quad (24)$$

$$\theta = \alpha \left[ e^{-(r-\xi)^2/\beta^2} + e^{-(r+\xi)^2/\beta^2} \right] \quad (25)$$

with  $r^2 = x^2 + y^2$  in plane polar coordinates. In this radially symmetric case the nematicon is ring-shaped (two-humped in 1D cross-sections), with a volcano-like form. Typical NLC cells are planar, but are relatively thick, so the assumption of radial symmetry is a good approximation as in experiments the sizes of both light beam and waveguide are much less than the cell width/thickness, so the influence of the planar boundaries on is minor. We then consider a sample cell with a radius  $R$  and  $R \gg \xi$ , an assumption tested in previous work with the outer value  $R$  taken as half the cell thickness versus  $y$ , which gave excellent agreement with experimental results [34].

The radially symmetric temperature equation (12) has the homogeneous solutions  $\ln r$  and a constant. As for (1 + 1)D, since the diffusivity  $\mu$  is large, we assume that the temperature within the circular peak of the nematicon is constant and decays as the homogeneous solution away from the axis, giving

$$\tau = \begin{cases} \tau_0, & 0 \leq r \leq \xi, \\ \tau_1 \ln \frac{R}{r}, & \xi < r < R \end{cases} \quad (26)$$

on using the boundary condition  $\tau = 0$  at  $r = R$ . Integrating the temperature equation (12) with  $u$  given by the trial function (24) from  $r = 0$  to  $r = R$  yields

$$\begin{aligned} \mu r \frac{\partial \tau}{\partial r} \Big|_{r=R} &= -a^2 w \left[ \frac{\sqrt{\pi}}{\sqrt{2}} \xi \operatorname{erf} \left( \frac{\sqrt{2}\xi}{w} \right) + w e^{-2\xi^2/w^2} \right] \\ &\sim -a^2 w \left[ \frac{\sqrt{\pi}}{\sqrt{2}} \xi + \frac{1}{2} w e^{-2\xi^2/w^2} \right] \end{aligned} \quad (27)$$

on using the asymptotic expansion of the error function for large argument to two terms [47]. Matching this derivative at  $r = R$  with the solution form (26) provides

$$\begin{aligned} \tau_1 &= \frac{a^2 w}{\mu} \left[ \frac{\sqrt{\pi}}{\sqrt{2}} \xi \operatorname{erf} \left( \frac{\sqrt{2}\xi}{w} \right) + w e^{-2\xi^2/w^2} \right] \\ &\sim \frac{a^2 w}{\mu} \left[ \frac{\sqrt{\pi}}{\sqrt{2}} \xi + \frac{1}{2} w e^{-2\xi^2/w^2} \right], \end{aligned} \quad (28)$$

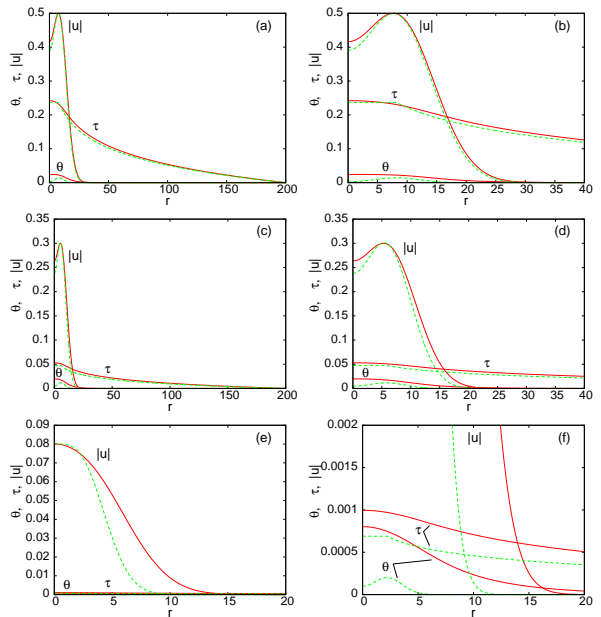


FIG. 3: Comparison between the (2 + 1)D thermo-reorientational solitary wave given by solutions of NLC equations (10)–(12) and those of the (2 + 1)D modulation equations (B1)–(B5). Solution of nematic equations: red (full) line; modulation solution: green (dashed) line. (a) Amplitude  $a = 0.5$ , with detailed view in (b), (c) amplitude  $a = 0.3$ , with detailed view in (d), (e)  $a = 0.08$ , with detailed view in (f). Here,  $\nu = 200$ ,  $\mu = 300$ ,  $q = 2$  and  $\gamma = 3.0$ .

again using the asymptotic expansion of the error function [47]. Continuity at  $r = \xi$  finally yields

$$\begin{aligned} \tau_0 &= \frac{a^2 w}{\mu} \left[ \frac{\sqrt{\pi}}{\sqrt{2}} \xi \operatorname{erf} \left( \frac{\sqrt{2}\xi}{w} \right) + w e^{-2\xi^2/w^2} \right] \ln \frac{R}{\xi} \\ &\sim \frac{a^2 w}{\mu} \left[ \frac{\sqrt{\pi}}{\sqrt{2}} \xi + \frac{1}{2} w e^{-2\xi^2/w^2} \right] \ln \frac{R}{\xi}. \end{aligned} \quad (29)$$

As well as the exact expression, the asymptotic form of  $\tau_0$  for large  $\xi$ ,  $\xi \ll R$ , has been given.

Having determined the 2D temperature distribution, the averaged Lagrangian can be calculated from the Lagrangian (16) based on the trial functions (24) and (25) with similar assumptions as for the (1+1)D averaged Lagrangian (23). Integrating the Lagrangian (16) in polar coordinates from  $r = 0$  to  $r = R$ , which is approximated as  $r = \infty$  due to the cell being much wider than the light beam, and in the polar angle from 0 to  $2\pi$ ,



results in the averaged Lagrangian

$$\begin{aligned}
\frac{1}{4\pi}\mathcal{L} = & -\sigma'a^2w \left[ we^{-\psi_w^2} + \frac{\sqrt{\pi}}{\sqrt{2}}\xi \operatorname{erf}(\psi_w) \right] \\
& - \frac{1}{2}a^2 \left[ 2e^{-\psi_w^2} - 2\frac{\xi^2}{w^2}e^{-\psi_w^2} + \frac{\sqrt{\pi}}{\sqrt{2}}\frac{\xi}{w} \operatorname{erf}(\psi_w) \right] \\
& - \frac{1}{2}\nu\alpha^2 \left[ 2e^{-\psi_\beta^2} - 2\frac{\xi^2}{\beta^2}e^{-\psi_\beta^2} + \frac{\sqrt{\pi}}{\sqrt{2}}\frac{\xi}{\beta} \operatorname{erf}(\psi_\beta) \right] \\
& - q\alpha^2\beta \left[ \beta e^{-\psi_\beta^2} + \frac{\sqrt{\pi}}{\sqrt{2}}\xi \operatorname{erf}(\psi_\beta) \right] \\
& + \frac{2f(\tau_0)\alpha a^2\beta^2 w^2}{2\beta^2 + w^2} \left[ 4e^{-\psi_1^2} + \sqrt{\pi}\psi_1 \operatorname{erf}(\psi_1) \right. \\
& + \sqrt{\pi}\psi_2 e^{-\frac{8\xi^2}{2\beta^2+w^2}} \operatorname{erf}(\psi_2) \\
& \left. + 2\sqrt{\pi}\psi_3 e^{-\frac{4(\beta^2+w^2)\xi^2}{w^2(2\beta^2+w^2)}} \operatorname{erf}(\psi_3) \right]. \quad (30)
\end{aligned}$$

Here, the arguments of the error functions are

$$\begin{aligned}
\psi_w = \frac{\sqrt{2}\xi}{w}, \quad \psi_\beta = \frac{\sqrt{2}\xi}{\beta}, \quad \psi_1 = \frac{\sqrt{2\beta^2+w^2}\xi}{\beta w}, \\
\psi_2 = \frac{(2\beta^2-w^2)\xi}{\beta w\sqrt{2\beta^2+w^2}}, \quad \psi_3 = \frac{w\xi}{\beta\sqrt{2\beta^2+w^2}}. \quad (31)
\end{aligned}$$

The variational equations obtained from this averaged Lagrangian are presented in Appendix B.

Figure 2 displays an example of a ring-shaped thermo-reorientational solitary wave solution of the (2 + 1) dimensional NLC equations (10)–(12), with a volcano shape, for the electric field amplitude  $a = 0.5$ , obtained using the ITEM. The electric field, temperature and director show the overall forms assumed in the derivation of the modulation equations, particularly the temperature  $\tau$  as given by (26). The beam has a bell shape, as in Fig. 2(a), with a crater on axis, as in Fig. 2(b), with a constant phase across it. Since the nonlocality parameter  $\nu$  is large,  $\nu = 200$ , the director appears single-peaked, as in (1 + 1)D, see Fig. 2(d), and does not mirror the volcano-shaped beam. Finally, the long logarithmic decay of the temperature from its peak as compared with the beam and the director is seen in Fig. 2(c), as in the solution (26) for the temperature. This markedly different decay of the director distribution and the temperature is important for the accurate description of thermo-reorientational nematicons. As stated in the Introduction, the functional forms of the competing focusing and defocusing contributions in the model equation (1), and its (2 + 1)D extension, are often assumed to be the same for analytical convenience. This is not adequate for real media, in particular for nematic liquid crystals.

Figure 3 compares (2 + 1)D radially symmetric solutions of the NLC equations (10)–(12) obtained from ITEM and those from the modulation equations (B1)–(B5), as for the (1 + 1)D comparisons of Fig. 1. The results resemble those in (1 + 1)D. The (1 + 1)D

and (2 + 1)D averaged Lagrangians, (23) and (30), respectively, and the modulation equations of Appendices A and B are broadly similar, so this is not unexpected. In analogy with (1+1)D, as the beam intensity decreases, the thermo-reorientational solitary wave evolves from a ring to a one-hump wavepacket. This occurs at an amplitude 0.14 according to the full numerical solution and at 0.105 for the modulation equations based on the parameter values given in the caption to Fig. 3. The various comparisons in Fig. 3 show this transition as the beam intensity/amplitude decreases. Clearly, the match between numerical and modulation solutions for the electric field  $|u|$  and temperature  $\tau$  of the ring shaped nematicons of Figs. 3(a)–(d) is excellent, with the modulation solution crater slightly deeper than that from numerical solutions. Nevertheless, the agreement between the solutions for the single peak nematicon of Figs. 3(e) and (f) is worse than that for the equivalent (1 + 1)D case of Figs. 1(e) and (f), due to the violation of the assumption of wavepacket peaks well separated from the origin. In addition, the modulation theory gives  $\xi \sim 2.2$ , which is much less than the  $\xi \sim 5.5$  for the (1 + 1)D case of Figs. 1(e) and (f), so that, again, the modulation solution does not satisfy the basic assumption used to derive the modulation equations (B1)–(B5). As in the (1 + 1)D case of Section III, the key modulation equation for the existence of a volcano-shaped thermo-reorientational nematicon is (B5), the variational equation obtained from variations  $\delta\xi$  of the averaged Lagrangian (30). To obtain a volcano solution with  $\xi \neq 0$ , in fact  $\xi$  sufficiently bounded above 0, the thermal contribution must be strong enough, in particular  $\partial f(\tau_0)/\partial\xi$  needs be sufficiently large and positive, to ensure a balance between the terms of positive and negative signs in this equation. This qualitative result reinforces the detailed conclusions from Fig. 3 on the need for a sufficiently strong defocusing for supermode solitary waves to exist.

The agreement for the director  $\theta$  is not as satisfactory, but more markedly so than for the (1 + 1)D case of Section III. Besides the role of the large nonlocality  $\nu$ , as in (1 + 1) dimensions, there is the extra effect of the deeper crater in the modulation solution. The optical forcing of the director is lower near  $r = 0$  and so is the reorientational response. In addition, the less accurate director distribution in (1 + 1) and (2 + 1) dimensions is connected with the trial functions (18) and (25) having two individual responses due to the two beams in the trial functions (17) and (24). The radial spreading in two transverse directions enhances this deeper crater, making an improved trial function for the director a requirement in (2 + 1) dimensions. This research effort is indeed underway as part of a systematic study of structured two dimensional self-confined light beams.

## V. CONCLUSIONS

The formation of multi-humped nematicons in  $(1 + 1)$ D and ring peaked, volcano shaped-nematicons in  $(2 + 1)$ D has been investigated in thermo-reorientational nematic liquid crystals by seeking steady solitary waves as numerical solutions of the governing equations, as well as solutions from modulation theory based on suitable trial functions in a variational formulation of the governing model. At variance with previous work, the physical reorientational and opto-thermal responses of NLC to extraordinary waves were employed in this study, rather than simplified models which do not model real media. The adopted equations consist of an NLS-type equation for the light beam and elliptic equations for both the molecular orientation and thermal responses. The variational solutions based on the modulation equations for the thermo-reorientational nematicons resulted in excellent agreement with the numerical solutions. In addition, we presented the first derived

$(2 + 1)$ D results on volcano-shaped nematicons. This is a remarkable result because of the lack of exact solitary wave solutions for the NLC equations [48], either with or without the competing defocusing contribution of relevance here, and also because the full physical medium responses were successfully incorporated. More work along this path is forthcoming towards investigating two-dimensional self-localized beam solutions with additional azimuthal features and their stability in symmetric, as well as non-symmetric, configurations. The theoretical tools developed hereby are expected to play an important role in analyzing other self-localized structured beams stemming from opposite/competing nonlinear responses in NLC, as well as, e. g., metal nanoparticle suspensions [49], photorefractive crystals [50], ferroelectric/photovoltaic crystals with counteracting photocurrents [51, 52], non-centrosymmetric crystals with a quadratic response [53], atomic vapours [54] and metamaterials [55], to mention only a few.

- 
- [1] M. Peccianti and G. Assanto, “Nematicons,” *Phys. Rep.*, **516**, 147–208 (2012).
- [2] G. Assanto, “Nematicons: reorientational solitons from optics to photonics,” *Liq. Cryst. Rev.*, **6**, 170–194 (2018).
- [3] M. Peccianti, G. Assanto, A. De Luca, C. Umeton and I. C. Khoo, “Electrically assisted self-confinement and waveguiding in planar nematic liquid crystal cells,” *Appl. Phys. Lett.*, **77**, 7–9 (2000).
- [4] G. B. Whitham, *Linear and Nonlinear Waves*, J. Wiley and Sons, New York (1974).
- [5] G. Assanto and N. F. Smyth, “Self-confined light waves in nematic liquid crystals,” *Physica D*, **402**, 132182 (2020).
- [6] C. Conti, M. Peccianti and G. Assanto, “Route to nonlocality and observation of accessible solitons,” *Phys. Rev. Lett.*, **91**, 073901 (2003).
- [7] Y. S. Kivshar and G.P. Agrawal, *Optical Solitons. From Fibers to Photonic Crystals*, Academic Press, San Diego (2003).
- [8] O. Bang, W. Krolikowski, J. Wyller and J. J. Rasmussen, “Collapse arrest and soliton stabilization in nonlocal nonlinear media,” *Phys. Rev. E*, **66**, 046619 (2002).
- [9] C. Conti, M. Peccianti and G. Assanto, “Observation of optical spatial solitons in a highly nonlocal medium,” *Phys. Rev. Lett.*, **92**, 113902 (2004).
- [10] J. M. L. MacNeil, N. F. Smyth and G. Assanto, “Exact and approximate solutions for optical solitary waves in nematic liquid crystals,” *Physica D*, **284**, 1–15 (2014).
- [11] S. Slussarenko, A. Alberucci, C.-P. Jisha, P. Piccirillo, E. Santamato, G. Assanto and L. Marrucci, “Guiding light via geometric phases,” *Nature Photon.*, **10**, 571–575 (2016).
- [12] M. A. Karpierz, M. Sierakowski, M. Swillo and T. Wolinski, “Self focusing in liquid crystalline waveguides,” *Mol. Cryst. Liq. Cryst.*, **320**, 157–163 (1998).
- [13] M. A. Karpierz, “Solitary waves in liquid crystalline waveguides,” *Phys. Rev. E*, **66**, 036603 (2002).
- [14] G. Assanto and N. F. Smyth, “Spin-optical solitons in liquid crystals,” *Phys. Rev. A*, **102**, 033501 (2020).
- [15] B. K. Esbensen, M. Bache, O. Bang and W. Krolikowski, “Anomalous interaction of nonlocal solitons in media with competing nonlinearities,” *Phys. Rev. A*, **86**, 033838 (2012).
- [16] S. Pu, M. Chen, Y. Li and L. Zhang, “Solitons in liquid crystals with competing nonlinearities,” *Opt. Commun.*, **450**, 78–86 (2019).
- [17] I. S. Jung, M. A. Karpierz, M. Trippenbach, D. N. Christodoulides and W. Krolikowski, “Supermode spatial solitons via competing nonlocal nonlinearities,” *Photon. Lett. Pol.*, **10**, 33–35 (2018).
- [18] A. Ramaniuk, M. Trippenbach, P. S. Jung, D. N. Christodoulos, W. Krolikowski and G. Assanto, “Scalar and vector supermode solitons owing to competing nonlocal nonlinearities,” *Opt. Express*, **29**, 8015–8023 (2021).
- [19] P. S. Jung, W. Krolikowski, U. A. Laudyn, M. Trippenbach and M. A. Karpierz, “Supermode spatial optical solitons in liquid crystals with competing nonlinearities,” *Phys. Rev. A*, **95**, 023820 (2017).
- [20] P. S. Jung, W. Krolikowski, U. A. Laudyn, M. A. Karpierz and M. Trippenbach, “Semi-analytical approach to supermode spatial solitons formation in nematic liquid crystals,” *Opt. Express*, **25**, 23893 (2017).
- [21] Y. Du, Z. Zhou, H. Tian and D. Liu, “Bright solitons and repulsive in-phase interaction in media with competing nonlocal Kerr nonlinearities,” *J. Opt.*, **13**, 015201 (2011).
- [22] M. Warengem, J. F. Blach and J. F. Henninot, “Thermo-nematicon: an unnatural coexistence of solitons in liquid crystals?,” *J. Opt. Soc. Amer. B*, **25**, 1882–1887 (2008).
- [23] U. A. Laudyn, A. Piccardi, M. Kwasny, M. A. Karpierz and G. Assanto, “Thermo-optic soliton routing in nematic liquid crystals,” *Opt. Lett.*, **43**, 2296–2299 (2018).
- [24] U. A. Laudyn, A. Piccardi, M. Kwasny, M. A. Karpierz

- and G. Assanto, “Thermo-optic soliton routing in nematic liquid crystals: erratum,” *Opt. Lett.*, **44**, 2268–2269 (2019).
- [25] K. Cyprych, P. S. Jung, Y. Izdebskaya, V. Shvedov, D. N. Christodoulides and W. Krolikowski, “Anomalous interaction of spatial solitons in nematic liquid crystals,” *Opt. Lett.*, **44**, 267–270 (2019).
- [26] U. A. Laudyn, M. Kwasny, A. Piccardi, M. A. Karpierz, R. Dabrowski, O. Chojnowska, A. Alberucci and G. Assanto, “Nonlinear competition in nematicon propagation,” *Opt. Lett.*, **40**, 5235–5238 (2015).
- [27] A. Alberucci, U. A. Laudyn, A. Piccardi, M. Kwasny, B. Klus, M. A. Karpierz and G. Assanto, “Nonlinear continuous-wave optical propagation in nematic liquid crystals: interplay between reorientational and thermal effects,” *Phys. Rev. E*, **96**, 012703 (2017).
- [28] U. A. Laudyn, A. Piccardi, M. Kwasny, B. Klus, M. A. Karpierz and G. Assanto, “Interplay of thermo-optic and reorientational responses in nematicon generation,” *Materials*, **11**, 1837 (2018).
- [29] Y. V. Izdebskaya, V. G. Shvedov, P. S. Jung and W. Krolikowski, “Stable vortex soliton in nonlocal media with orientational nonlinearity,” *Opt. Lett.*, **43**, 66–69 (2018).
- [30] M. Kwaśny, M. A. Karpierz, G. Assanto and U. A. Laudyn, “Optothermal vortex-solitons in liquid crystals,” *Opt. Lett.*, **45**, 2451–2453 (2020).
- [31] A. A. Minzoni, N. F. Smyth and A. L. Worthy, “Modulation solutions for nematicon propagation in non-local liquid crystals,” *J. Opt. Soc. Amer. B*, **24**, 1549–1556 (2007).
- [32] B. Malomed, “Variational methods in nonlinear fiber optics and related fields,” *Prog. Opt.*, **43**, 71–193 (2002).
- [33] G. Assanto, *Nematicons, Spatial Optical Solitons in Nematic Liquid Crystals*, John Wiley and Sons, New York (2012).
- [34] G. Assanto, C. Khan, A. Piccardi and N. F. Smyth, “Temperature control of nematicon trajectories,” *Phys. Rev. E*, **100**, 062702 (2019).
- [35] J. Yang and T. I. Lakoba, “Accelerated imaginary-time evolution methods for the computation of solitary waves,” *Stud. Appl. Math.*, **120** 265–292 (2008).
- [36] J. J. García-Ripoll and V. M. Pérez-García, “Optimizing Schrödinger functionals using Sobolev gradients: applications to quantum mechanics and nonlinear optics,” *SIAM J. Scien. Comput.*, **23**, 1316–1334 (2001).
- [37] J. Yang, “Newton-conjugate-gradient methods for solitary wave computations,” *J. Comp. Phys.*, **228**, 7007–7024 (2009).
- [38] I. Khoo, *Liquid Crystals: Physical Properties and Nonlinear Optical Phenomena*, John Wiley and Sons (2007).
- [39] B. D. Skuse and N. F. Smyth, “Interaction of two colour solitary waves in a liquid crystal in the nonlocal regime,” *Phys. Rev. A*, **79**, 063806 (2009).
- [40] D. J. Kaup and A. C. Newell, “Solitons as particles, oscillators, and in slowly changing media: a singular perturbation theory,” *Proc. Roy. Soc. Lond. A*, **361**, 413–446 (1978).
- [41] B. D. Skuse and N. F. Smyth, “Interaction of two colour solitary waves in a liquid crystal in the nonlocal regime,” *Phys. Rev. A*, **79**, 063806 (2009).
- [42] G. Assanto, N. F. Smyth and A. L. Worthy, “Two colour, nonlocal vector solitary waves with angular momentum in nematic liquid crystals,” *Phys. Rev. A*, **78**, 013832 (2008).
- [43] S. A. Louis, T. R. Marchant and N. F. Smyth, “Optical solitary waves in thermal media with non-symmetric boundary conditions,” *J. Phys. A: Math. Gen.*, **46**, 055201 (2013).
- [44] S. A. Louis, T. R. Marchant and N. F. Smyth, “2-D solitary waves in thermal media with nonsymmetric boundary conditions,” *Stud. Appl. Math.*, **142**, 586–607 (2019).
- [45] C. G. Broyden, “A class of methods for solving nonlinear simultaneous equations,” *Math. Comput.*, **19**, 577–593 (1965).
- [46] W. H. Press, S. A. Teukolsky, W. T. Vetterling and B. P. Flannery, *Numerical Recipes in Fortran 77. The Art of Scientific Computing*, Press Syndicate, University of Cambridge, Cambridge (1992).
- [47] M. Abramowitz and I. A. Stegun, *Handbook of Mathematical Functions with Formulas, Graphs, and Mathematical Tables*, National Bureau of Standards, Washington, D.C. (1964).
- [48] G. Assanto, A. A. Minzoni and N. F. Smyth, “Light self-localization in nematic liquid crystals: modelling solitons in nonlocal reorientational media,” *J. Nonlin. Opt. Phys. Mater.*, **18**, 657–691 (2009).
- [49] A. Balbuena-Ortega, F. E. Torres-González, V. López-Gayou, R. Delgado-Macuil, J. E. H. Cardoso-Sakamoto, A. V. Arzola, G. Assanto and K. Volke-Sepulveda, “Guiding light with singular beams in nanoplasmonic colloids,” *Appl. Phys. Lett.*, **118**, 061102 (2021).
- [50] J. Feinberg, “Asymmetric self-defocusing of an optical beam from the photorefractive effect,” *J. Opt. Soc. Am.*, **72**, 46–51 (1982).
- [51] J. Safioui, F. Devaux, K. P. Huy and M. Chauvet, “High intensity behavior of pyroelectric photorefractive self-focusing in  $LiNbO_3$ ,” *Opt. Commun.*, **294**, 294–298 (2013).
- [52] F. Devaux, J. Safioui, M. Chauvet and R. Passier, “Two-photoactive-center model applied to photorefractive self-focusing in biased  $LiNbO_3$ ,” *Phys. Rev. A*, **81**, 013825 (2010).
- [53] F. Setzpfandt, D. Neshev, R. Schiek, F. Lederer, A. Tünnermann and T. Pertsch, “Competing nonlinearities in quadratic nonlinear waveguide arrays,” *Opt. Lett.*, **34**, 3589–3591 (2009).
- [54] F. Maucher, T. Pohl, S. Skupin and W. Krolikowski, “Self-organization of light in optical media with competing nonlinearities,” *Phys. Rev. Lett.*, **116**, 163902 (2016).
- [55] P. V. Kapitanova, A. P. Slobozhnyuk, I. V. Shadrivov, P. A. Belov and Y. S. Kivshar, “Competing nonlinearities with metamaterials,” *Appl. Phys. Lett.*, **101**, 231904 (2012).

#### Appendix A: (1 + 1)D modulation equations

The modulation (variational) equations obtained from the (1 + 1)D averaged Lagrangian (23) determining the

thermo-reorientational nematics are

$$\begin{aligned} & \left\{ \frac{\nu}{\beta} \left[ 1 + \left( 1 - 4 \frac{\xi^2}{\beta^2} \right) e^{-2\xi^2/\beta^2} \right] \right. \\ & \left. + 2q\beta \left[ 1 + e^{-2\xi^2/\beta^2} \right] \right\} \alpha \\ & = \frac{4a^2\beta w}{\sqrt{2}\sqrt{2\beta^2+w^2}} \left\{ 1 + e^{-\frac{8\xi^2}{2\beta^2+w^2}} + 2e^{-\frac{4(\beta^2+w^2)\xi^2}{w^2(2\beta^2+w^2)}} \right. \\ & \left. + \gamma\tau_0 \left[ 2 + e^{-\frac{4(\beta^2+w^2)\xi^2}{w^2(2\beta^2+w^2)}} \right] \right\}, \quad (\text{A1}) \end{aligned}$$

$$\begin{aligned} & 2\sqrt{2}w \left[ 1 + e^{-2\xi^2/w^2} \right] \sigma' \\ & = -\frac{\sqrt{2}}{w} \left[ 1 + \left( 1 - 4 \frac{\xi^2}{w^2} \right) e^{-2\xi^2/w^2} \right] \\ & + \frac{8\alpha\beta w}{\sqrt{2\beta^2+w^2}} \left[ 1 + e^{-\frac{8\xi^2}{2\beta^2+w^2}} + 2e^{-\frac{4(\beta^2+w^2)\xi^2}{w^2(2\beta^2+w^2)}} \right] \\ & + \frac{8\gamma\tau_0\alpha\beta w}{\sqrt{2\beta^2+w^2}} \left[ 2 + e^{-\frac{4(\beta^2+w^2)\xi^2}{w^2(2\beta^2+w^2)}} \right] \\ & + \frac{4\gamma\alpha\beta w}{\sqrt{2\beta^2+w^2}} \frac{\partial\tau_0}{\partial a} \left[ 2 + e^{-\frac{4(\beta^2+w^2)\xi^2}{w^2(2\beta^2+w^2)}} \right], \quad (\text{A2}) \end{aligned}$$

$$\begin{aligned} 0 & = -2\sqrt{2}\sigma' \left[ 1 + \left( 1 + \frac{4\xi^2}{w^2} \right) e^{-2\xi^2/w^2} \right] \\ & + \frac{\sqrt{2}}{w^2} \left[ 1 + \left( 1 - 16 \frac{\xi^2}{w^2} + 16 \frac{\xi^4}{w^4} \right) e^{-2\xi^2/w^2} \right] \\ & + \frac{16\alpha\beta^3}{(2\beta^2+w^2)^{3/2}} \left[ 1 + e^{-\frac{8\xi^2}{2\beta^2+w^2}} + 2e^{-\frac{4(\beta^2+w^2)\xi^2}{w^2(2\beta^2+w^2)}} \right] \\ & + \frac{128\alpha\beta w^2\xi^2}{(2\beta^2+w^2)^{5/2}} \left[ e^{-\frac{8\xi^2}{2\beta^2+w^2}} \right. \\ & \left. + \left( 1 + 2 \frac{\beta^2}{w^2} + 2 \frac{\beta^4}{w^4} \right) e^{-\frac{4(\beta^2+w^2)\xi^2}{w^2(2\beta^2+w^2)}} \right] \\ & + \frac{64\gamma\tau_0\alpha\beta\xi^2}{w^2(2\beta^2+w^2)^{5/2}} \left( w^4 + 2\beta^2w^2 + 2\beta^4 \right) e^{-\frac{4(\beta^2+w^2)\xi^2}{w^2(2\beta^2+w^2)}} \\ & + \frac{8\gamma\alpha\beta w}{\sqrt{2\beta^2+w^2}} \frac{\partial\tau_0}{\partial w} \left[ 2 + e^{-\frac{4(\beta^2+w^2)\xi^2}{w^2(2\beta^2+w^2)}} \right], \quad (\text{A3}) \end{aligned}$$

$$\begin{aligned} 0 & = 2\sqrt{2}\frac{a^2}{w}\sigma'\xi e^{-2\xi^2/w^2} + \sqrt{2}\frac{a^2\xi}{w^3} \left( 3 - 4 \frac{\xi^2}{w^2} \right) e^{-2\xi^2/w^2} \\ & + \sqrt{2}\frac{\nu\alpha^2\xi}{\beta^3} \left( 3 - 4 \frac{\xi^2}{\beta^2} \right) e^{-2\xi^2/\beta^2} + 2\sqrt{2}q\frac{\alpha^2\xi}{\beta} e^{-2\xi^2/\beta^2} \\ & - \frac{32\alpha a^2 w \beta \xi}{(2\beta^2+w^2)^{3/2}} \left[ e^{-\frac{8\xi^2}{2\beta^2+w^2}} + \frac{\beta^2+w^2}{w^2} e^{-\frac{4(\beta^2+w^2)\xi^2}{w^2(2\beta^2+w^2)}} \right] \\ & - \frac{16\gamma\tau_0\alpha a^2 \beta \xi (\beta^2+w^2)}{w(2\beta^2+w^2)^{3/2}} e^{-\frac{4(\beta^2+w^2)\xi^2}{w^2(2\beta^2+w^2)}} \\ & + \frac{2\gamma\alpha a^2 \beta w}{\sqrt{2\beta^2+w^2}} \frac{\partial\tau_0}{\partial \xi} \left[ 2 + e^{-\frac{4(\beta^2+w^2)\xi^2}{w^2(2\beta^2+w^2)}} \right], \quad (\text{A4}) \end{aligned}$$

$$\begin{aligned} 0 & = \sqrt{2}\nu\frac{\alpha}{\beta^2} \left[ 1 + \left( 1 - 16 \frac{\xi^2}{\beta^2} + 16 \frac{\xi^4}{\beta^4} \right) e^{-2\xi^2/\beta^2} \right] \\ & - 2\sqrt{2}q\alpha \left[ 1 + \left( 1 + \frac{4\xi^2}{\beta^2} \right) e^{-2\xi^2/\beta^2} \right] \\ & + \frac{8a^2w^3}{(2\beta^2+w^2)^{3/2}} \left[ 1 + e^{-\frac{8\xi^2}{2\beta^2+w^2}} + 2e^{-\frac{4(\beta^2+w^2)\xi^2}{w^2(2\beta^2+w^2)}} \right] \\ & + \frac{64a^2\beta^2w\xi^2}{(2\beta^2+w^2)^{5/2}} \left[ 2e^{-\frac{8\xi^2}{2\beta^2+w^2}} + e^{-\frac{4(\beta^2+w^2)\xi^2}{w^2(2\beta^2+w^2)}} \right] \\ & + \frac{8\gamma\tau_0a^2w^3}{(2\beta^2+w^2)^{5/2}} \left[ 2 + e^{-\frac{4(\beta^2+w^2)\xi^2}{w^2(2\beta^2+w^2)}} \right] \\ & + \frac{64\gamma\tau_0a^2\beta^2w\xi^2}{(2\beta^2+w^2)^{5/2}} e^{-\frac{4(\beta^2+w^2)\xi^2}{w^2(2\beta^2+w^2)}}, \quad (\text{A5}) \end{aligned}$$

The modulation equations (A1) and (A2) give solutions for the director response amplitude  $\alpha$  and the phase  $\sigma'$ , respectively, so that only the three modulation equations (A3)–(A5) are solved using Broyden's method [45, 46].

## Appendix B: (2 + 1)D modulation equations

The variational equations obtained from the (2 + 1)D averaged Lagrangian (30) are highly involved. The attraction of variational methods is the ability to obtain approximate solutions which are simple enough to analyze to determine the behavior of propagating beams in various scenarios. For this reason, the limit of the averaged Lagrangian for the ring peak well separated from the origin  $r = 0$ , which is the case for the nematicon solutions presented here, will be taken. This approximation is consistent with the approximation (26) for the temperature. We thus expand the error functions in the averaged Lagrangian (30) to two terms in their asymptotic expansions for large argument [47]. The modulation, or variational equations, obtained from the averaged Lagrangian (30) in this limit are then

$$\begin{aligned} & \left\{ \nu \left[ \frac{\sqrt{\pi}}{\sqrt{2}} \frac{\xi}{\beta} + \left( \frac{3}{2} - \frac{2\xi^2}{\beta^2} \right) e^{-\frac{2\xi^2}{\beta^2}} \right] \right. \\ & \left. + 2q\beta \left[ \frac{\sqrt{\pi}}{\sqrt{2}} \xi + \frac{1}{2}\beta e^{-\frac{2\xi^2}{\beta^2}} \right] \right\} \alpha \\ & = \frac{2\sqrt{\pi}f(\tau_0)a^2\beta w\xi}{(2\beta^2+w^2)^{3/2}} \left[ 2\beta^2+w^2 + (2\beta^2-w^2) e^{-\frac{8\xi^2}{2\beta^2+w^2}} \right. \\ & \left. + 2w^2 e^{-\frac{4(\beta^2+w^2)\xi^2}{w^2(2\beta^2+w^2)}} \right], \quad (\text{B1}) \end{aligned}$$

$$\begin{aligned}
& 2\sigma' \left[ \frac{\sqrt{\pi}}{\sqrt{2}} \xi w + \frac{1}{2} w^2 e^{-\frac{2\xi^2}{w^2}} \right] \\
&= - \left[ \frac{\sqrt{\pi}}{\sqrt{2}} \frac{\xi}{w} + \left( \frac{3}{2} - \frac{2\xi^2}{w^2} \right) e^{-\frac{2\xi^2}{w^2}} \right] \\
&+ \frac{2\sqrt{\pi}\alpha\beta w\xi}{\sqrt{2\beta^2+w^2}} \left[ 2f(\tau_0) + a \frac{\partial f(\tau_0)}{\partial a} \right] \\
&+ \frac{2\sqrt{\pi}\alpha\beta w\xi}{(2\beta^2+w^2)^{3/2}} \left( 2f(\tau_0) + a \frac{\partial f(\tau_0)}{\partial a} \right) \times \\
&\left[ (2\beta^2-w^2) e^{-\frac{8\xi^2}{2\beta^2+w^2}} + 2w^2 e^{-\frac{4(\beta^2+w^2)\xi^2}{w^2(2\beta^2+w^2)}} \right], \quad (\text{B2})
\end{aligned}$$

$$\begin{aligned}
0 &= -\sigma' \left[ \frac{\sqrt{\pi}}{\sqrt{2}} \xi + w \left( 1 + \frac{2\xi^2}{w^2} \right) e^{-\frac{2\xi^2}{w^2}} \right] \\
&- \frac{1}{2} \left[ -\frac{\sqrt{\pi}}{\sqrt{2}} \frac{\xi}{w^2} + \left( \frac{3}{2} + \frac{10\xi^2}{w^3} - \frac{8\xi^4}{w^5} \right) e^{-\frac{2\xi^2}{w^2}} \right] \\
&+ \frac{4\sqrt{\pi}f(\tau_0)\alpha\beta^3\xi}{(2\beta^2+w^2)^{3/2}} + \frac{2\sqrt{\pi}\alpha\beta w\xi}{\sqrt{2\beta^2+w^2}} \frac{\partial f(\tau_0)}{\partial w} \\
&+ \frac{4\sqrt{\pi}f(\tau_0)\alpha\beta\xi(\beta^2-w^2)}{(2\beta^2+w^2)^{5/2}} \left[ (2\beta^2-w^2) e^{-\frac{8\xi^2}{2\beta^2+w^2}} \right. \\
&\left. + 2w^2 e^{-\frac{4(\beta^2+w^2)\xi^2}{w^2(2\beta^2+w^2)}} \right] \\
&+ \frac{2\sqrt{\pi}\alpha\beta w\xi}{(2\beta^2+w^2)^{3/2}} \frac{\partial f(\tau_0)}{\partial w} \left[ (2\beta^2-w^2) e^{-\frac{8\xi^2}{2\beta^2+w^2}} \right. \\
&\left. + 2w^2 e^{-\frac{4(\beta^2+w^2)\xi^2}{w^2(2\beta^2+w^2)}} \right] \\
&+ \frac{4\sqrt{\pi}f(\tau_0)\alpha\beta w^2\xi}{(2\beta^2+w^2)^{3/2}} \left[ \left( -1 + \frac{8(2\beta^2-w^2)\xi^2}{(2\beta^2+w^2)^2} \right) e^{-\frac{8\xi^2}{2\beta^2+w^2}} \right. \\
&\left. + 2 \left( 1 - \frac{4\beta^2\xi^2}{(2\beta^2+w^2)^2} \right) e^{-\frac{4(\beta^2+w^2)\xi^2}{w^2(2\beta^2+w^2)}} \right], \quad (\text{B3})
\end{aligned}$$

$$\begin{aligned}
0 &= -\frac{1}{2}\nu\alpha \left[ -\frac{\sqrt{\pi}}{\sqrt{2}} \frac{\xi}{\beta^2} + \left( \frac{3}{2} + \frac{10\xi^2}{\beta^3} - \frac{8\xi^4}{\beta^5} \right) e^{-\frac{2\xi^2}{\beta^2}} \right] \\
&- q\alpha \left[ \frac{\sqrt{\pi}}{\sqrt{2}} \xi + \beta \left( 1 + \frac{2\xi^2}{\beta^2} \right) e^{-\frac{2\xi^2}{\beta^2}} \right] + \frac{2\sqrt{\pi}f(\tau_0)a^2w^3\xi}{(2\beta^2+w^2)^{3/2}} \\
&+ \frac{2\sqrt{\pi}f(\tau_0)a^2w\xi(w^2-4\beta^2)}{(2\beta^2+w^2)^{5/2}} \left[ (2\beta^2-w^2) e^{-\frac{8\xi^2}{2\beta^2+w^2}} \right. \\
&\left. + 2w^2 e^{-\frac{4(\beta^2+w^2)\xi^2}{w^2(2\beta^2+w^2)}} \right] \\
&+ \frac{8\sqrt{\pi}f(\tau_0)a^2\beta^2w\xi}{(2\beta^2+w^2)^{3/2}} \left[ e^{-\frac{8\xi^2}{2\beta^2+w^2}} \right. \\
&+ \frac{8(2\beta^2-w^2)\xi^2}{(2\beta^2+w^2)^2} e^{-\frac{8\xi^2}{2\beta^2+w^2}} \\
&\left. + \frac{4w^2\xi^2}{(2\beta^2+w^2)^2} e^{-\frac{4(\beta^2+w^2)\xi^2}{w^2(2\beta^2+w^2)}} \right], \quad (\text{B4})
\end{aligned}$$

$$\begin{aligned}
0 &= -\sigma'a^2 \left[ \frac{\sqrt{\pi}}{\sqrt{2}} w - 2\xi e^{-\frac{2\xi^2}{w^2}} \right] \\
&- \frac{1}{2}a^2 \left[ \frac{\sqrt{\pi}}{\sqrt{2}} \frac{1}{w} - \left( \frac{3}{2} + \frac{10\xi}{w^2} - \frac{8\xi^3}{w^4} \right) e^{-\frac{2\xi^2}{w^2}} \right] \\
&- \frac{1}{2}\nu\alpha^2 \left[ \frac{\sqrt{\pi}}{\sqrt{2}} \frac{1}{\beta} - \left( \frac{3}{2} + \frac{10\xi}{\beta^2} - \frac{8\xi^3}{\beta^4} \right) e^{-\frac{2\xi^2}{\beta^2}} \right] \\
&- q\alpha^2 \left[ \frac{\sqrt{\pi}}{\sqrt{2}} \beta - 2\xi e^{-\frac{2\xi^2}{\beta^2}} \right] \\
&+ \frac{2\sqrt{\pi}\alpha a^2\beta w}{\sqrt{2\beta^2+w^2}} \left[ f(\tau_0) + \xi \frac{\partial f(\tau_0)}{\partial \xi} \right] \\
&+ \frac{2\sqrt{\pi}\alpha a^2\beta w}{(2\beta^2+w^2)^{3/2}} \left[ (2\beta^2-w^2) e^{-\frac{8\xi^2}{2\beta^2+w^2}} \right. \\
&\left. + 2w^2 e^{-\frac{4(\beta^2+w^2)\xi^2}{w^2(2\beta^2+w^2)}} \right] \left[ f(\tau_0) + \xi \frac{\partial f(\tau_0)}{\partial \xi} \right] \\
&- \frac{32\sqrt{\pi}f(\tau_0)\alpha a^2\beta w\xi^2}{(2\beta^2+w^2)^{5/2}} \left[ (2\beta^2-w^2) e^{-\frac{8\xi^2}{2\beta^2+w^2}} \right. \\
&\left. + (\beta^2+w^2) e^{-\frac{4(\beta^2+w^2)\xi^2}{w^2(2\beta^2+w^2)}} \right]. \quad (\text{B5})
\end{aligned}$$

As for the (1+1)D modulation equations, the variational Eq. (B1) determines the director amplitude  $\alpha$  and the modulation equation Eq. (B2) the nematic phase  $\sigma'$ , so that only the three modulation equations Eqs. (B3)–(B5) need to be solved using Broyden's Method.

The use of modulation theory has been pushed to its useful limits given the involved nature of the (1+1) and (2+1) dimensional modulation equations. To extend modulation theory to solitary waves with more than two humps, which means three or more interacting component beams, requires better choices of trial functions with the requisite number of peaks. The alternative is the use of numerical solutions only.